J Neurophysiol 94: 775–787, 2005.
First published March 9, 2005; doi:10.1152/jn.01093.2004.

Cortical Maps of Separable Tuning Properties Predict Population Responses to Complex Visual Stimuli

Tanya I. Baker[1] and Naoum P. Issa[2]

[1]*Department of Physics and* [2]*Department of Neurobiology, Pharmacology, and Physiology, University of Chicago, Chicago, Illinois*

Submitted 18 October 2004; accepted in final form 5 March 2005

Baker, Tanya I., and Naoum P. Issa. Cortical maps of separable tuning properties predict population responses to complex visual stimuli. *J Neurophysiol* 94: 775–787, 2005. First published March 9, 2005; doi:10.1152/jn.01093.2004. In the earliest cortical stages of visual processing, a scene is represented in different functional domains selective for specific features. Maps of orientation and spatial frequency preference have been described in the primary visual cortex using simple sinusoidal grating stimuli. However, recent imaging experiments suggest that the maps of these two spatial parameters are not sufficient to describe patterns of activity in different orientation domains generated in response to complex, moving stimuli. A model of cortical organization is presented in which cortical temporal frequency tuning is superimposed on the maps of orientation and spatial frequency tuning. The maps of these three tuning properties are sufficient to describe the activity in orientation domains that have been measured in response to drifting complex images. The model also makes specific predictions about how moving images are represented in different spatial frequency domains. These results suggest that the tangential organization of primary visual cortex can be described by a set of maps of separable neuronal receptive field features including maps of orientation, spatial frequency, and temporal frequency tuning properties.

INTRODUCTION

In the classic description of the organization of primary visual cortex, repeating modules, or hypercolumns, encode all the parameters needed to represent a small portion of a visual stimulus (Hubel and Wiesel 1977). Within each hypercolumn, information about the orientation, spatial frequency, and drift direction of image components is encoded by overlapping groups of neurons (Bonhoeffer and Grinvald 1991; Hubel and Wiesel 1977; Hubener et al. 1997; Issa et al. 2000; Shmuel and Grinvald 1996; Weliky et al. 1996). These hypercolumns tile the cortical surface, making interlacing maps of response properties.

However, other than direction, these parameters give no information about image motion. In a recent experiment, Basole et al. (2003) showed that changing the temporal properties of a moving image can change which orientation domains are activated by the image. These shifts in orientation responses cannot be predicted from the cortical organization of spatial parameters such as orientation and spatial frequency preference alone. This suggests that the classic description of cortical organization is not sufficient to describe the distributed responses of the cortex to moving images.

The response properties of primary visual cortex are important determinants of how moving images are perceived. For example, it is hypothesized that the tuning properties of V1 cells limit dynamic acuity (Levi 1996). Similarly, the perception of motion streaks that trail a quickly moving image seems to be encoded in the firing pattern of V1 neurons (Geisler 1999; Geisler et al. 2001). To understand how motion is encoded in the visual cortex, both spatial and temporal response properties must be characterized. The spatio-temporal energy model of human motion vision has been used as a framework for characterizing the response properties of individual cortical neurons (Adelson and Bergen 1985; DeAngelis et al. 1993b; De Valois et al. 1979; Gizzi et al. 1990; McLean and Palmer 1989; van Santen and Sperling 1985; Watson and Ahumada 1985). Two stages of processing constitute the spatio-temporal energy model. The first stage is a linear filtering of image properties including orientation, spatial frequency, and temporal frequency. In the second stage, the outputs of the first stage are combined in quadrature to remove phase-sensitivity from neuronal responses. Recently, the spatio-temporal energy model has been suggested as an appropriate framework for characterizing the organization of cortical maps (Basole et al. 2003; Mante and Carandini 2003).

In this paper we describe the functional organization of the primary visual cortex in terms of the linear filters of the spatio-temporal energy model and present it in the context of the hypercolumn model. We show that the distributed pattern of activity in the cortex generated in response to moving, complex images can be characterized by three maps of separable tuning properties: orientation, spatial frequency, and temporal frequency tuning. This model is sufficient to quantitatively predict the activity patterns previously measured in response to moving complex images (Basole et al. 2003). In addition, it predicts transitions in the responses of different spatial frequency domains that might underlie specific psychophysical phenomena.

METHODS

Model overview

We use a series of three linear filters to model the population responses of primary visual cortex, similar to the first stage of the spatio-temporal energy models proposed for human motion perception (Adelson and Berger 1985; van Santen and Sperling 1985; Watson and Ahumada 1985). These filters can be described by six separable tuning properties: orientation preference and bandwidth, spatial frequency preference and bandwidth, and temporal frequency preference and bandwidth. In this formulation, only a subset of image components is represented by neural activity. Image components

Address for reprint requests and other correspondence: Naoum P. Issa, 947 E. 58th St., MC0926, Dept. of Neurobiology, Pharmacology, and Physiology, Univ. of Chicago, Chicago, IL 60637 (E-mail: nissa@drugs.bsd.uchicago.edu).

The costs of publication of this article were defrayed in part by the payment of page charges. The article must therefore be hereby marked "*advertisement*" in accordance with 18 U.S.C. Section 1734 solely to indicate this fact.

whose spatial frequency and/or temporal frequency fall outside the band-pass of the spatio-temporal filters of primary visual cortex are not encoded by neural activity.

According to this model, the spatial pattern of cortical activity induced by a stimulus depends on how these six parameters are organized. We will present simulations for four different spatial arrangements; each layout is representative of a different region of V1, a different species, or a different developmental stage.

In the simplest arrangement, only orientation preference varies within a hypercolumn. Preliminary reports and recently published low-resolution maps suggest that this might be the case in ferret Area 17 (Basole et al. 2004; Schwartz 2003; Yu et al. 2002). On this small spatial scale, spatial frequency and temporal frequency tuning properties are assumed to be constant. A map of orientation preference is combined with a single spatial frequency tuning curve and a single temporal frequency tuning curve to simulate population responses. We compare the results of simulations of this cortical layout to data from measurements made over a small region of ferret Area 17 in response to drifting bar textures (Basole et al. 2003).

In the second arrangement, we assume a gradual change in the preferred spatial frequency over several millimeters of cortex, consistent with the variation in retinal sampling density with eccentricity (Basole et al. 2004). As in the first arrangement, we assume there is little to no change within a hypercolumn. Maps of orientation and spatial frequency preference and a single temporal frequency tuning curve are used to predict how orientation domains at different eccentricities respond to moving images.

The third arrangement simulates responses within cat Area 17. As in the previous case, maps of orientation and spatial frequency preference combined with a single temporal frequency tuning curve are used to make predictions about cortical response patterns. However, in this case, the spatial frequency map varies within a hypercolumn. There have been differing descriptions of the organization of spatial frequency preference in cat Area 17 (Everson et al. 1998; Hubener et al. 1997; Issa et al. 2000; Shoham et al. 1997; Tolhurst and Thompson 1982; Tootell et al. 1981), but all share the common finding that spatial frequency preference varies systematically within the space of a hypercolumn. We use one of the proposed layout of spatial frequency preference (Issa et al. 2000) as an example, but our simulations do not rely on a specific configuration—all that is required is that spatial frequency preference varies on a small spatial scale.

Finally we consider the layout in which temporal frequency preference varies in conjunction with spatial frequency preference. While temporal frequency preference does not seem to depend on spatial frequency preference in young cats, there is a clear dependence in Area 17 of adult cats (Baker 1990; DeAngelis et al. 1993a). Both extracellular recording and intrinsic signal imaging experiments suggest an inverse relationship between spatial frequency and temporal frequency preference (Baker 1990; DeAngelis et al. 1993a; Shoham et al. 1997).

Spatio-temporal filters

The three filters are described by standard orientation, spatial frequency, and temporal frequency tuning curves. The tuning curves are defined by Gaussians as

$$S(p) = \exp\left(-\frac{[\log_2(p) - \log_2(S_p)]^2}{2\sigma_S^2} \right) \quad (1)$$

$$T(\rho) = \exp\left(-\frac{[\log_2(\rho) - \log_2(T_p)]^2}{2\sigma_T^2} \right) \quad (2)$$

$$\Omega(\phi) = \exp\left(-\frac{[\phi - \tilde{\phi}]^2}{2\sigma_\Omega^2} \right) \quad (3)$$

where p is the spatial frequency coordinate, ϕ the orientation coordinate, and ρ the temporal frequency coordinate. Each tuning curve is characterized by a peak value and a width. In *Eq. 1*, S_p is the peak spatial frequency, and σ_S is proportional to the spatial frequency bandwidth. In *Eq. 2*, T_p is the peak temporal frequency, and σ_T is proportional to the temporal frequency bandwidth. The orientation tuning curve (*Eq. 3*) is defined as a wrapped Gaussian, with a peak orientation of $\tilde{\phi}$ and a characteristic width of σ_Ω.

For ease of simulation, all the tuning curves and stimuli are calculated in spatial frequency space. However, this is not a global spatial frequency transform. Each functional domain is treated as though it has a spatio-temporal receptive field. The spatial frequency and orientation tuning curves define an effective receptive field size and orientation for each functional domain (reviewed in Dayan and Abbott 2001): the width of the effective receptive field is inversely proportional to the spatial frequency bandwidth (σ_S), whereas the length of the receptive field is proportional to the ratio of the width and the orientation bandwidth (σ_Ω). The orientation of the receptive field is the same as the peak of the orientation tuning curve. Similarly, the temporal frequency tuning curve of a domain defines the temporal receptive field properties.

We simulate responses to rigid motion of an image (that is, all the components of the image move with the same velocity). The temporal frequency of each image component (ρ_i) can be determined from its spatial frequency and the drift velocity of the image along the orientation of the image component

$$\rho_i(v,\phi_d,p,\phi) = p \cdot v \cdot |\cos(\phi - \phi_d)| \quad (4)$$

where v is the drift speed of the stimulus, ϕ_d is the drift angle of the image, p is the spatial frequency of the image component, and ϕ is the orientation of the image component defined as orientation in spatial frequency coordinates, so a vertical grating has an orientation of 0° (see Fig. 1). The absolute value is taken because we ignore direction selectivity. Substituting this expression for ρ in *Eq. 2* gives the projection of the temporal frequency tuning curve onto the spatial frequency plane.

While the temporal frequency tuning curve is a property of neurons and is not stimulus dependent, its representation in spatial frequency coordinates does depend on the stimulus. *Eq. 4* shows how the transformation from temporal frequency coordinates to spatial frequency coordinates depends on stimulus motion parameters. For a given drift speed and angle, a restricted range of spatial frequencies have temporal frequencies in the temporal band-pass of the neuron. The projection of the temporal frequency tuning curve in the spatial frequency plane shows this range.

Population responses, R, within a functional domain (defined as small region of cortex that has a given set of orientation, spatial frequency and temporal frequency preferences) are modeled as the integral over all spatial frequencies and orientations of the stimulus, scaled by the spatial frequency, temporal frequency, and orientation tuning curves

$$R(v,\phi_d) = \int_{-\pi}^{\pi} \int_{0}^{\infty} A(p,\phi) \cdot S(p) \cdot \Omega(\phi) \cdot T(v,\phi_d,p,\phi) p \, dp d\phi \quad (5)$$

in which A is the amplitude of the stimulus component at spatial frequency p and ϕ. By reducing the variables to spatial frequency and orientation, *Eq. 5* allows one to visualize the effects of three separable filters in two dimensions.

In our analysis, we have limited stimuli to objects in an image moving at a single velocity. However, it can be generalized to account for several objects moving at different speeds and directions. Because it is a linear model, responses in a functional domain to a stimulus consisting of objects with different velocities would be determined by a summation of its responses to each object individually

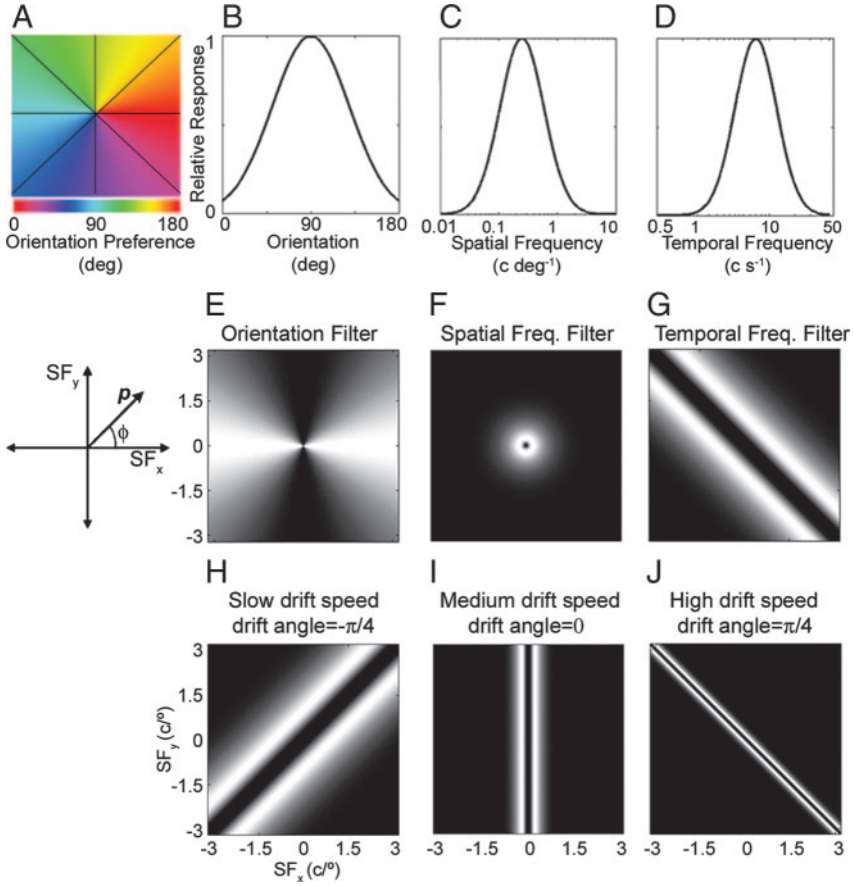

FIG. 1. Organization of filtering properties within a single hypercolumn of ferret V1. *A*: only orientation preference changes systematically within a hypercolumn. Orientation preference is organized in a pinwheel arrangement and is color-coded in the standard method used to display orientation maps. Iso-orientation lines are shown in black; all the pixels along a line have the same orientation preference. *B*: orientation tuning curve for a pixel in the 90° orientation domain. *C*: spatial frequency tuning curve with a peak at 0.25 c/°. *D*: temporal frequency tuning curve with a peak at 7 c/s. *E*: representation of the orientation tuning curve in *B* in spatial frequency coordinates. Axes represent spatial frequency along the *x* dimension (SF_x, shown to the diagram to the left) and *y* dimension (SF_y). *F*: representation of the spatial frequency filter in *C* in spatial frequency coordinates. *G*: representation of temporal frequency tuning curve shown in *D* in spatial frequency coordinates for a stimulus drifting at an angle of $\pi/4$ rad and at a speed of 10°/s. *H–J*: effects of changing drift angle and speed on the projection of temporal frequency tuning curve onto the spatial frequency plane. Temporal frequency tuning curves shown for drift angles of $-\pi/4$ (*H*), 0 (*I*), and $\pi/4$ radians (*J*) and drift speeds of 10 (*H*), 30 (*I*), and 70°/s (*J*).

$$R = \sum_{i=1}^{N} \int_{-\pi}^{\pi} \int_{0}^{\infty} A_i(p,\phi) \cdot S(p) \cdot \Omega(\phi) \cdot T(v_i,\phi_{di},p,\phi) p \, dp d\phi \qquad (6)$$

in which there are *N* objects (each of whose spatial Fourier transform is represented by A_i) moving at velocities $\boldsymbol{v}_i = (v_i,\phi_{di})$.

An equivalent way of calculating these responses is to keep the temporal frequency coordinate in the model. The net response in a domain would then be given by

$$R = \int_{0}^{\infty} \int_{-\pi}^{\pi} \int_{0}^{\infty} A(p,\phi,\rho) \cdot S(p) \cdot \Omega(\phi) \cdot T(\rho) p \, dp d\phi d\rho \qquad (7)$$

in which *A* is now the temporal and spatial Fourier transform of the stimulus. This generalized representation can be used to simulate responses within a functional domain to more complex moving images. It is useful to note that the model is equivalent to the convolution of the stimulus image with a spatio-temporal receptive field, with the assumption that the receptive field is spatio-temporally separable. For a stimulus centered in the receptive field, the function $S(p)\Omega(\phi)$ is the spatial Fourier transform of the spatial component of the receptive field, and the function $T(\rho)$ is the temporal Fourier transform of the temporal component of the receptive field.

Simulations

We simulated responses in functional domains to complex stimuli moving through the visual field. Stimuli are presented over 80 × 80° (full field), which is represented in a 512 × 512 pixel array (0.157°/pixel). To represent the stimuli in terms of their spatial frequency components, the two-dimensional spatial Fourier transform is taken (Fig. 2). Likewise, the tuning curves are represented in the two-dimensional spatial Fourier plane, as shown in Fig. 1. The integral shown in *Eq. 5* is solved numerically by summing over a 3.2 cycles/deg range of spatial frequencies. In Figs. 3–6 and 9, 90° have been added to ϕ to give orientation domains as often defined by responses to oriented gratings (that is, horizontal grating have an orientation of 0° and vertical bars have an orientation of 90°).

Parameter values for the tuning curves are taken from optical and electrophysiological measurements in the ferret and cat (Table 1). Parameters for cat Area 17 were taken from optical imaging experiments (Zhang and Issa 2004) and are similar to the values reported electrophysiologically (Movshon et al. 1978). We estimated the average temporal frequency preference (T_p), spatial frequency bandwidth (σ_S), and temporal frequency bandwidth (σ_T) for ferret Area 17 from fits to the data of Basole et al. (2003).

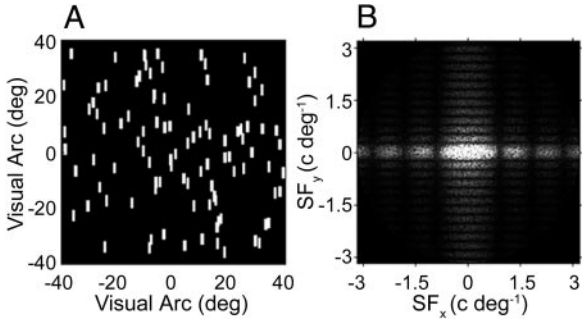

FIG. 2. A sample stimulus. *A*: sample bar-texture stimulus consisting of 100 randomly placed 1 × 4° bars oriented vertically. Axis units are in degrees of visual space. *B*: spatial Fourier representation of stimulus shown in *A*. Each point represents one sinusoidal grating component of texture stimulus. Axis units are in c/°.

TABLE 1. *Tuning parameters in cat Area 17 (optical measurements; Zhang and Issa 2004) and in ferret Area 17*

Parameter	Cat	Ferret—Hypercolumn	Ferret—Long Range Maps
Orientation preference (ϕ)	Varies point-by-point between 0 and 180°	Varies point-by-point between 0 and 180°	Varies point-by-point between 0 and 180°
Orientation bandwdith (σ_Ω)	40° (Rao et al. 1997)	40° (Issa et al. 1999; Rao et al. 1997)	40° (Issa et al. 1999; Rao et al. 1997)
Spatial frequency preference (S_p)	Varies point-by-point between 0.2 and 1.5 c/° Population average: 0.44 c/°	0.25 c/° (Baker et al. 1998)	0.15 to 0.3 c/° (Basole et al. 2004)
Spatial frequency bandwidth (σ_S)	Individual SF domains: 0.91 ± 0.07 c/° Population average: 1.63 ± 0.20 c/°	1.25 c/°*	1.25 c/°*
Temporal frequency preference (T_p)	Constant TF model: 2.23 ± 0.41 c/s Varying TF model: SF $<$ 0.8: TF = -3.7 SF + 4.1 SF $>$ 0.8: TF = 1.15 (DeAngelis et al. 1993a)	6–7 c/s*	6–7c/s*
Temporal frequency bandwidth (σ_T)	2.73 ± 0.43 c/s	0.8 c/s*	0.8 c/s*

Values are means ± SE. σ is the characteristic width of the tuning curves. *Parameters were estimated from fits of the model to the data of Basole et al. (2003) but see Alitto and Usrey (2004).

RESULTS

Model predictions

Can linear spatio-temporal filtering account for the distributed pattern of cortical activity produced in response to complex, moving images? To address this question, we first compared the predictions of the spatio-temporal filtering model to measurements made in ferret primary visual cortex of activity driven by drifting texture stimuli (Basole et al. 2003). Assuming that only orientation preference varies across a hypercolumn, the simulations provide a quantitative description of the orientation domain activation patterns observed in the ferret cortex (Basole et al. 2003). We generalized this approach to other cortical areas by incorporating the organization of different parameters, such as spatial frequency and temporal frequency tuning. This model is used to make predictions about the qualitative differences in response patterns that cortical areas with different organizations should have.

Activity patterns in a hypercolumn in which only orientation preference varies

To test the spatio-temporal filtering model, we compared simulation results to measurements made in the ferret visual cortex by Basole et al. (2003). Because the measurements of Basole et al. (2003) were made over a small area of cortex, we restricted simulations to a region containing just one or a few hypercolumns. On this scale, orientation preference is arrayed in pinwheels (Chapman et al. 1996; Rao et al. 1997; Weliky et al. 1995), and we assumed that spatial frequency preference does not change substantially (schematized in Fig. 1, *A–D*).

The responses of an orientation domain to a moving image can be predicted from the domain's spatial and temporal filtering properties. Individually, the spatio-temporal filters can be represented by the tuning curves for orientation, spatial frequency, and temporal frequency (Fig. 1, *B–D*). To visualize the predicted activity patterns, we will display the tuning curves in spatial Fourier coordinates (Fig. 1, *E–G*). Both the spatial frequency tuning curve and the orientation tuning curve have simple representations in the spatial Fourier plane: each depends on only one of the polar axes of the spatial Fourier plane, p (spatial frequency), or ϕ (orientation; see Fig. 1, *E* and *F*).

The representation of the temporal frequency filter in the spatial Fourier plane may be less intuitive. Because a rigid object moves through a visual scene at a single velocity, the temporal frequency of each component of the image is proportional to its spatial frequency: components with high spatial frequencies move with higher temporal frequencies than do components with low spatial frequencies (*Eq. 4*). As a result, the temporal frequency tuning curve of a domain limits the range of spatial frequencies that it can encode.

In a slowly moving image, a component can have any of a wide range of spatial frequencies and still have a temporal frequency within the temporal band-pass of the neuron. For example, the bright regions in Fig. 1*H* show the range of spatial frequencies that fall within the temporal frequency tuning curve for an image moving at a slow speed of 10°/s. In comparison, a quickly moving image has a much narrower range of spatial frequencies that a component can have and still fall within the temporal frequency band-pass; 70°/s drift speed (Fig. 1*J*). Because the temporal frequency tuning curve can be projected onto the spatial frequency plane, we can visualize how changing temporal properties of a stimulus can affect responses in different domains of primary visual cortex. In the following four sub-sections, we explore how specific changes in image drift velocity and the spatial statistics of an image affect the population responses in a small region of the ferret visual cortex.

DRIFT ANGLE. First we consider the effect of changing the stimulus drift angle on the population response. In this case, the spatial properties of the stimulus do not change. Figure 2*A* shows an example of the texture stimuli used in these simulations. Elongated bars that move with a fixed velocity are randomly distributed across the visual field. The spatial Fourier transform of the stimulus (Fig. 2*B*) shows that the components of the image cover a range of orientations and spatial frequencies. This distribution does not change with image motion. However, the temporal frequency of each component does depend on the drift angle, as given in *Eq. 4*. As a result, the

temporal frequency filter passes image components with different orientations depending on drift angle.

Figure 3 shows simulated responses in different orientation domains (orientation response curves) for four different drift angles of a texture stimulus. For motion perpendicular to the long axis of the bars, the texture activates the same orientation domains that would be activated by a grating of the same orientation (Fig. 3*A*, *top row*; Fig. 3*B*, solid line). For motion that is not perpendicular to the long axis of the bars, the orientation domain most strongly activated is not the same as the orientation of the bars.

Varying the drift angle changes which portion of the two-dimensional Fourier spectrum of the stimulus falls within the spatio-temporal tuning envelope of the neurons that make up the orientation domain. To show this, the activity in each of four orientation domains for four drift angles is shown in Fig. 3*A* (see also Supplementary Materials 1[1]). Each panel shows the product of all three tuning curves (as in Fig. 1, *E–G*) and the stimulus (Fig. 2*B*). The predicted response in an orientation domain is the integral of the filtered stimulus components over the spatial Fourier plane (*Eq. 5*). The brightness of the panel is proportional to the activity in the domain.

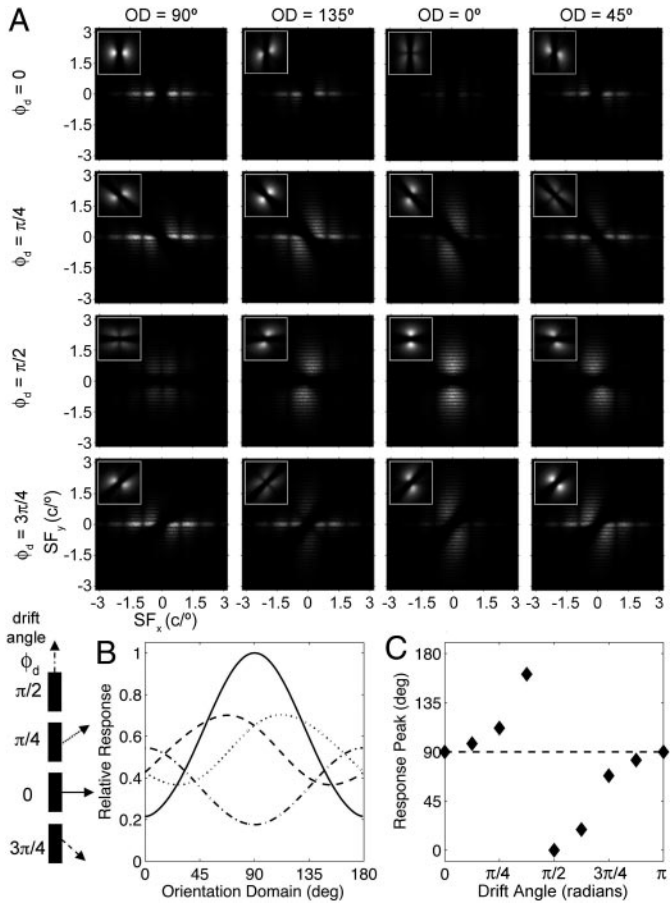

FIG. 3. Systematic shifts in the population response as image drift angle changes. Stimuli are texture patterns composed of vertical bars 1° wide and 6° long, drifting at 5°/s. *A*: each panel shows the product of the 3 spatio-temporal filters (as in Fig. 1, *E–G*) and the stimulus (as in Fig. 2*B*) in the spatial Fourier plane. *Insets*: product of spatio-temporal filters. Integral over the plane determines the amount activity in a given orientation domain; the brighter the panel, the more activity in the domain. Orientation domain, and therefore the shape of the orientation filter in spatial Fourier space, varies by column (OD, orientation domain). Drift angle, and therefore the shape of the temporal frequency tuning curve represented in the spatial Fourier plane, varies by row (ϕ_d, drift angle). *B*: simulated responses of different orientation domains in ferret Area 17, shown for stimuli at drifting each of 4 angles: 0 (horizontal drift, solid line), $\pi/4$ (dotted line), $\pi/2$ (dash-dot line), and $3\pi/4$ rad (dashed line). Points were calculated for each curve at 1° intervals. *C*: peak orientation response from response curves as in *B* with the textured pattern moving along 9 drift angles (0 to π radians at $\pi/8$ radian intervals).

For horizontal drift of vertical bars, the 90° orientation domain passes more of the power in the stimulus than does any other domain (compare the *top left panel* to the other panels in the *top row*). For a drift angle of $\pi/2$, the strongest response is in the 0° orientation domain. In the example shown in Fig. 3, a $\pi/4$ (45°) clockwise shift in the axis of motion changed the distribution of population activity such that it peaked at 68°. In a symmetrical fashion, a $\pi/4$ counterclockwise shift in texture motion evokes a response peaked at 112°.

As the drift angle changes, different image components are filtered out by the temporal frequency, spatial frequency, and orientation tuning curves. As Fig. 1, *H–J* and *Eq. 4* show, drift angle is one of the main factors that determines which image components fall within the temporal frequency band-pass of cortical neurons. The representation of the temporal frequency tuning curve in two-dimensional spatial Fourier coordinates is rotated by a change in the drift angle of the stimulus. With the rotation, the stimulus components that fall within the temporal and spatial frequency tuning curves have orientations that differ from the orientation of the long axis of the bars.

DRIFT SPEED. Changing the speed at which a stimulus drifts changes the peak orientation response (Basole et al. 2003). Figure 4*A* gives an impression of the effect of drift speed on responses in four orientation domains. At a slow drift speed (10 °/s), the peak response sits between 90 and 135°, as suggested by the nearly equal brightness of the two *top left panels*. It is more difficult to estimate by eye the peak orientation for high drift speeds (Fig. 4*A*, *bottom row*), but the numerical integral over each of the planes shows that the peak response is between 45 and 90°. The animation in Supplementary Materials 2[1] gives a better visual impression of how responses shift among orientation domains as a function of drift speed.

Consistent with the experimental findings of Basole et al. (2003), our simulations show that, for motion not orthogonal to the long edges of the bar, the peak response orientation changes smoothly with drift speed (Fig. 4). Again, the shift in orientation responses can be explained by changes in the projection of the temporal frequency tuning curve onto spatial frequency space (Fig. 1, *H–J*). As drift speed increases, the stimulus components that contribute to the response are limited to a narrower spatial frequency band along the direction of motion. Changing the drift speed alters which stimulus orientations fall within the temporal and spatial frequency tuning curves of the cortical area. This is in contrast to a full field grating stimulus whose image components are all of a single orientation; because no other orientations exist in the stimulus, there is no shift in the orientation domains that are activated as the drift velocity changes.

There is a unique drift speed (the crossing speed) at which the population response peaks at the dominant orientation of the texture (the long axis of the component bars). The value of the crossing speed depends on both the spatial and temporal

[1] The Supplementary Material for this article (four animations) is available online at http://jn.physiology.org/cgi/content/full/01093.2004/DC1.

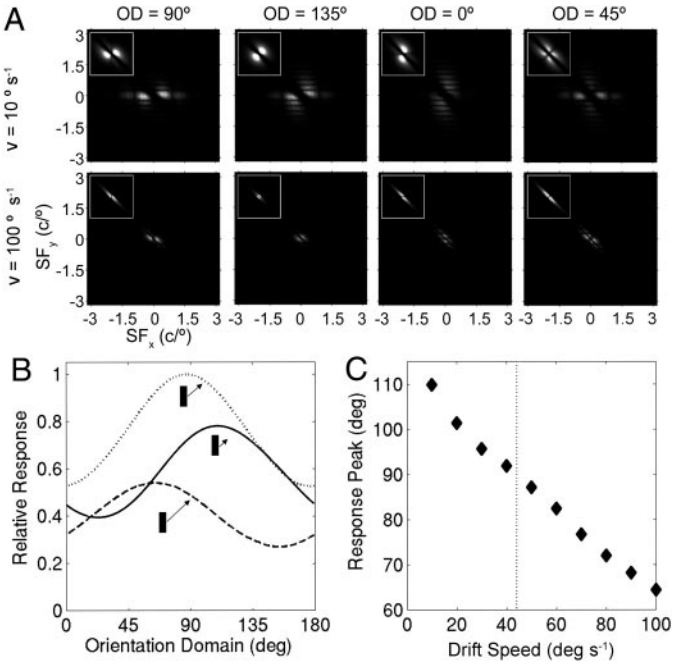

FIG. 4. Shifts in peak orientation as drift speed increases. Stimulus textures are $1 \times 4°$ vertical bars drifting at an angle of $\pi/4$ radians at various speeds. *A*: each panel shows the product of the 3 spatio-temporal tuning filters and stimulus in the spatial Fourier plane. *Insets*: product of filters only. Orientation domain, and therefore the shape of the orientation filter in spatial Fourier space, varies by column. Drift speed, and therefore the shape of the temporal frequency tuning curve in spatial Fourier space, varies by row. *B*: simulated population responses of ferret Area 17 for a texture stimulus moving at 10 (solid line), 50 (dotted line), and 100°/s (dashed line); peak orientation responses are at 110, 87, and 64°, respectively. *C*: peak orientation responses for texture stimulus drifting at speeds ranging from 10 to 100°/s at 10°/s intervals. Dotted line indicates the speed at which the peak orientation response matches orientation of the bars of the stimulus ($v = 44$°/s).

frequency tuning curves (as well as the aspect ratio). The crossing speed measured in the ferret primary visual cortex is about 45°/s [for $4 \times 1°$ vertical bars drifting at $\pi/4$ radians, see Fig. 3 in Basole et al. (2003)]. Given an average spatial frequency preference of 0.25 cycles/° (Baker et al. 1998), the crossing speed is consistent with a peak temporal frequency preference of 6 to 7 cycles/s (Fig. 4*C*).

The shift in peak orientation response is not always a smooth one. When the bars are so short that they are essentially dots, the transition at the crossing speed is abrupt: the peak response shifts from one orientation domain to the orthogonal orientation domain without going through intermediate orientations. Figure 5 shows the results of two simulations in which random dot fields drift at a speed on either side of the crossing speed. Consistent with the response profiles in supplementary Fig. 4 of Basole et al. (2003), slowly drifting dot fields activate orientation domains determined by the drift angle (the 135° orientation domain in Fig. 5), but at high speeds, the dot field activates the orthogonal orientation (the 45° orientation domain in Fig. 5).

ASPECT RATIO. The degree of shift in peak orientation response also depends on the aspect ratio of the bars that make up the texture. At one extreme, infinitely elongated bars approximate gratings and the stimulus has only one orientation, so only one orientation domain can be activated regardless of drift speed or angle (similar to the case shown in Fig. 6*A*, *bottom row*). At the other extreme, a field of randomly distributed dots has power distributed evenly over all orientations and (unevenly) over many spatial frequencies (similar to Fig. 6*A*, *top row*). In this case, the peak orientation is determined by the drift speed and angle of the texture field. For intermediate aspect ratios, the degree of shift is inversely related to the aspect ratio (Fig. 6*B*, Supplementary Materials 3[1]).

Figure 6 shows the effect of increasing bar length on the predicted shift in peak orientation response. The shift is greatest for dots and progressively decreases with increasing aspect ratio (Fig. 6*C*). The reduction in shift occurs whether the drift speed is greater than (Fig. 6*C*, ♦) or less than (Fig. 6*C*, ◇) the crossing speed.

In the simulations shown in Fig. 6*C*, the peak orientations do not asymptote at 90° with increasing aspect ratio, as might be expected by the fact that full field vertical gratings best activate the 90° orientation domain. Instead, for a drift speed of 5°/s, the peak response approaches an asymptote of 110° as bar length increases, and the response peak approaches 83° for a drift speed of 100°/s. The offset of the asymptotes from 90° is due to the short edges of the bars (at the orthogonal orientation) that drift across the visual field even when the bar length is longer than the full visual field. The peak orientation response would be 90° if none of the short edges of the bars drift through the field of vision. In our simulation this occurs once the stimulus bars reached a length twice the height of the visual field (160°).

Using the estimated ferret parameters, the population response evoked by a stimulus of vertical bars of length 2, 4, or 10° (and 1° wide) are peaked at 124, 117, and 109°, respectively, when the drift speed is 5°/s. Although these shifts are qualitatively similar to those seen in Fig. 2*A* of Basole et al. (2003), with the estimated ferret parameters, the model underestimates the shift with the shortest bars by about 10° and overestimates the shift by 5° for the longest bar [equivalent values in Fig. 2*A* of Basole et al. (2003) are 135, 119, and 104°].

SHIFTS WITH ORTHOGONAL MOTION. The smooth transitions among different orientation domains have all been observed for

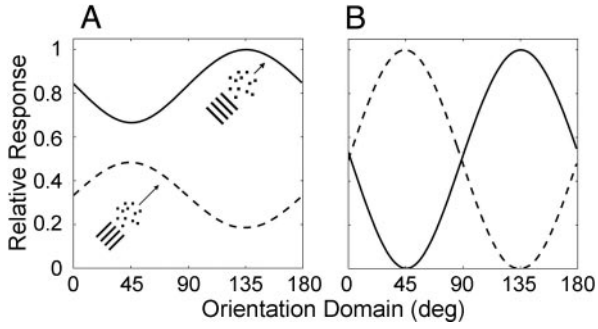

FIG. 5. Changing speed induces a shift in the population response to random dots. *A*: peak population response to random dot patterns shifts by 90° as drift speed increases from 20 (solid line) to 100°/s (dashed line). Stimulus texture consists of 300 squares, each 1° on a side, drifting at an angle of $\pi/4$ radians. Next to each trace is a schematic of the stimulus and its motion, with the length of the arrow proportional to speed. Below each texture pattern is the grating stimulus that would produce a similar response. *B*: mean of 2 curves has been made the same for comparison with imaging data, in which high-pass spatial filtering makes the mean intensity the same for all stimulus conditions. Simulations use estimated ferret Area 17 parameters with spatial frequency preference = 0.25c/°.

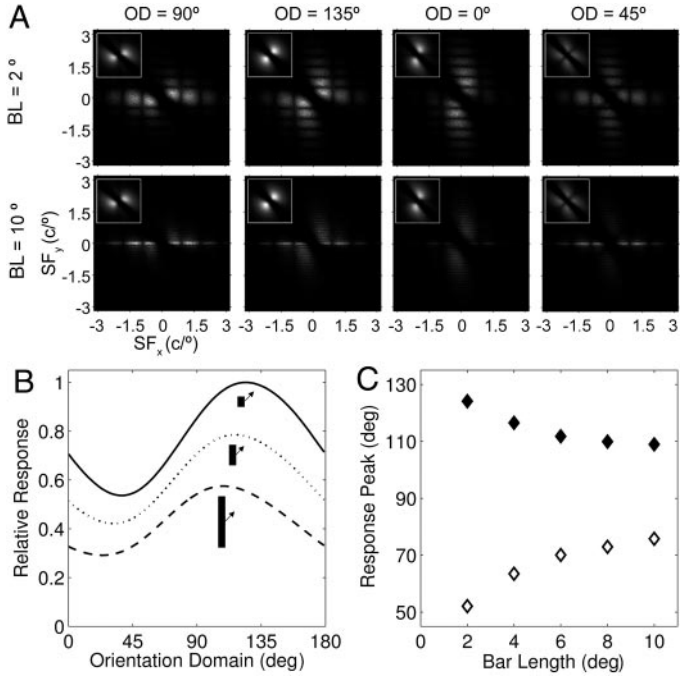

FIG. 6. Effect of bar length on the shift in peak orientation. *A*: product of the spatio-temporal tuning curves and stimulus in spatial Fourier space. Orientation domains vary by column, aspect ratio of the bars comprising the texture vary by row. For short bar lengths (BL = 2°, *top row*), stimulus has components distributed over all orientations, so the peak orientation of the response is determined primarily by the drift angle (peak orientation is close to 135°). For large aspect ratios (long bar length, BL = 10°, *bottom row*), most of the power in the stimulus is around a single orientation (vertical), so the peak orientation is determined primarily by the orientation of the long axis of the bars (peak orientation is close to 90°). *B*: simulated responses of different orientation domains in ferret Area 17 shown for texture stimuli consist of vertical bars 1° wide × 2 (solid black), 4 (dotted), or 10° (dashed) long. Stimulus is drifting with a speed of 5°/s at an angle of $\pi/4$ radians. Bar density was decreased while the bar length was increased to conserve mean luminance. *C*: peak orientation of responses obtained with a slow drift speed (5°/s, ♦) and from the same stimuli drifting at a high drift speed (100°/s, ◇) for bars of increasing length.

diagonal motion (motion not orthogonal to the long axis of the bars; Basole et al. 2003). However, the model also predicts transitions between orientation domains for orthogonal motion. For example, vertical bars drifting horizontally slowly should activate vertical orientation domains, but the same bars drifting quickly should activate horizontal orientation domains.

The speed at which this transition should occur depends both on the tuning properties of the cortex and on the characteristics of the stimulus. The transition speed increases as the aspect ratio of the bars increases (Fig. 7). For ferret Area 17 parameters, the transition for random dots is at 33°/s, but for bars with an aspect ratio of 4 the transition is around 70°/s. No such transition is predicted for gratings moving at various speeds.

Activity patterns at different eccentricities

While we assume spatial frequency preference is relatively constant on the scale of an orientation pinwheel in ferret V1, spatial frequency preference does seem to change over larger spatial scales (Basole et al. 2004; Schwartz 2003). In central visual fields, spatial frequency preference is higher than in peripheral visual fields (Basole et al. 2004; Schwartz 2003). This cortical arrangement is schematized in Fig. 8, in which

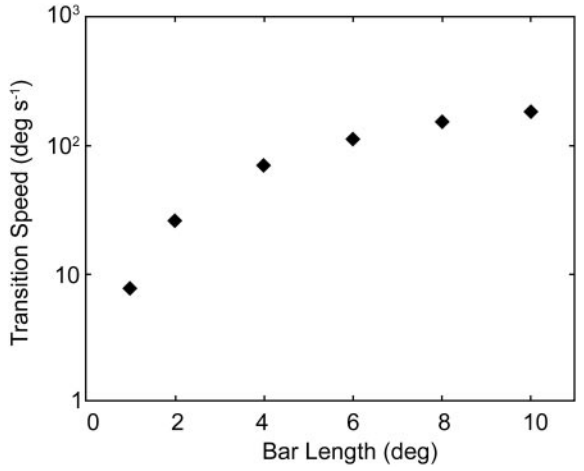

FIG. 7. Transition speed increases with the aspect ratio of the bars in a texture stimulus. Results are shown for ferret Area 17 (spatial frequency preference = 0.25 c/°). Stimulus textures are composed of bars 1° wide with the bar length indicated.

orientation preference repeats many times over several millimeters of cortex, but spatial frequency preference increases gradually and monotonically from the peripheral to the central visual field. The spatio-temporal filtering model predicts how transitions described in Figs. 3, 4, and 6 occur at different eccentricities. Simulation results are shown in Fig. 9.

There is no significant variation in population responses at different eccentricities for slowly drifting bars at various drift angles (Fig. 9*A*). However, the variation is enhanced with increasing drift speed. The higher spatial frequency preference in the central visual field causes the transitions in this zone should to be more sensitive to drift speed (Fig. 9*B*). High spatial frequency image components in an image move at comparatively high temporal frequencies. These image components exceed the temporal band-pass of the cortical neurons at slower drift speeds than do the low spatial frequency image components. As a result, high spatial frequency components with orientations different from the drift angle would be accentuated at relatively low drift speeds. This can be seen in the larger slope of peak orientation as a function of drift speed in high spatial frequency zones (Fig. 9*B*).

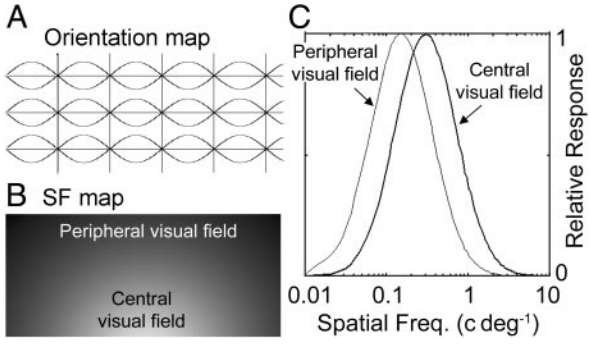

FIG. 8. Organization of filtering properties over large distances in ferret V1. *A*: orientation map over several millimeters of cortex is schematized by iso-orientation lines; the lines come together at orientation-pinwheel centers. *B*: spatial frequency preference changes gradually over the cortical surface, such that spatial frequency preference is relatively constant over the span of a single orientation pinwheel but varies between 0.15 and 0.3 c/° going from the peripheral to the central visual field. Spatial scale as in *A*. *C*: spatial frequency tuning curves for the central and peripheral visual fields are plotted.

Changing aspect ratios also differentially affects activity patterns in the central and peripheral regions of V1. At low drift speeds (below the crossing speed) these effects are subtle (Fig. 9*C*, filled symbols), but are accentuated at higher drift speeds (Fig. 9*C*, open symbols). As the aspect ratio of the bars in a texture increases, power is lost at all orientations other than the dominant one (the orientation of the long axis of the bars). Interestingly, the areas of low spatial frequency preference are more sensitive to this shift than the areas of high spatial frequency preference for high drift speeds. This can be attributed to the effect of the temporal frequency tuning curve which at high speeds filters out all high spatial frequency components except for a narrow band oriented orthogonal to the drift angle (see Supplementary Materials 3 and 4[1]).

The larger the difference in spatial frequency preference between cortical zones, the greater the effects outlined in Fig. 9. Because spatial frequency preference only varies by a factor of 2 over the dorsal part of ferret V1 (Basole et al. 2004), different locations should show only a small difference in the peak orientation of responses. A wider spread of spatial frequency preferences will produce more substantial differences in response patterns across spatial frequency domains.

Activity patterns within a hypercolumn of cat Area 17

In cat Area 17, spatial frequency preference varies systematically within the space of a hypercolumn (Everson et al. 1998; Hubener et al. 1997; Issa et al. 2000; Shoham et al. 1997; Tolhurst and Thompson 1982; Tootell et al. 1981). As a result, identifiable regions within a hypercolumn encode different combinations of stimulus orientation and spatial frequency. The layout shown in Fig. 10 summarizes the organization of spatial frequency preference as reported by Issa et al. (2000), in which the spatial frequency map is coupled to the orientation map.

The linear filtering model predicts how a change in the temporal properties of a stimulus should change the activation of cortical spatial frequency domains. An object moving through the visual field is composed of several spatial frequencies drifting at the same speed. The temporal frequency of each component is proportional to its spatial frequency (*Eq. 4*).

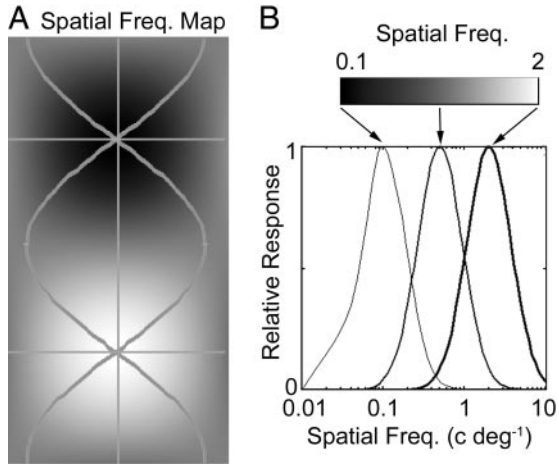

FIG. 10. Organization of filtering properties within a cat Area 17 hypercolumn, assuming that temporal frequency preference is constant. *A*: spatial frequency preference (grayscale) varies continuously within a hypercolumn. Superimposed on the spatial frequency map are iso-orientation lines. Two orientation pinwheels are shown, with their centers aligned with the peak and trough of the spatial frequency map. *B*: spatial frequency tuning curves for different locations in the spatial frequency map. Temporal frequency tuning curve is constant at different locations within the map (peak at 2.2 c/s, bandwidth of 2.7 c/s).

Assuming that the temporal frequency tuning curve is the same for all spatial frequency domains in the primary visual cortex, high spatial frequencies in a complex image should not be encoded at high drift speeds.

As an example, we compared the predicted responses to drifting sine wave and square wave gratings in different spatial frequency domains. A square wave grating is made up of a series sinusoidal components covering a range of spatial frequencies all at the same orientation. Each component of the drifting square wave grating has a different temporal frequency, and as the drift speed increases, the temporal frequencies increase. As Fig. 11, *C* and *D* shows, the high spatial frequency components of a slowly drifting square wave grating should effectively drive the visual cortex. With increasing speeds, however, the high spatial frequency components fall outside of the temporal frequency tuning curve. At high drift speeds, therefore, square wave gratings should not be distin-

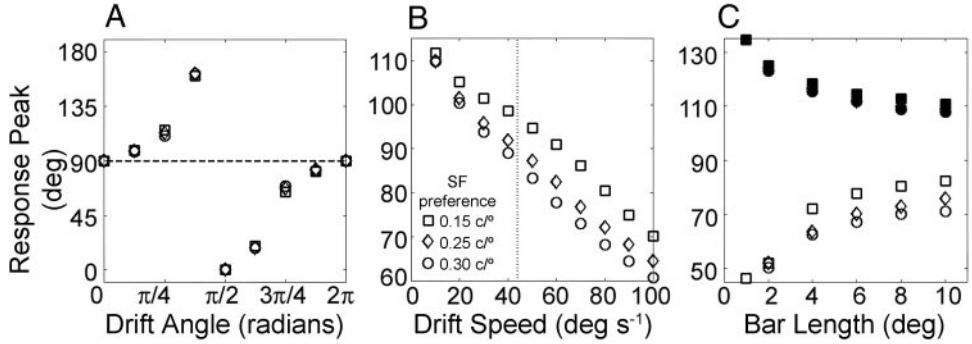

FIG. 9. Effect of eccentricity on predicted responses in the ferret visual cortex. Simulations as in Figs. 3, 4, and 6; results are reproduced here for comparison (diamonds). For all plots, responses are for population average with a spatial frequency preference of 0.25 c/° (diamonds), low spatial frequency areas (preference of 0.15 c/°; squares), and high spatial frequency areas (0.30 c/°; circles). *A*: shifts in the population response as image drift angle changes. Stimulus is a texture composed of 1 × 6° bars drifting at 5°/s the specified drift angle (as in Fig. 3*B*). In this case, responses do not significantly vary in areas of differing spatial frequency preference. *B*: as drift speed increases, orientation responses shift more in central visual field (high spatial frequency) than in peripheral visual field (low spatial frequency). Stimuli are composed of 1 × 4° bars and drift at an angle of $\pi/4$ radians (as in Fig. 4*B*). *C*: effect of bar length and spatial frequency preference on the shift in peak orientation. Responses to bars drifting at 5°/s indicated by filled symbols; responses to bars drifting at 100°/s indicated by open symbols (as in Fig. 6*B*).

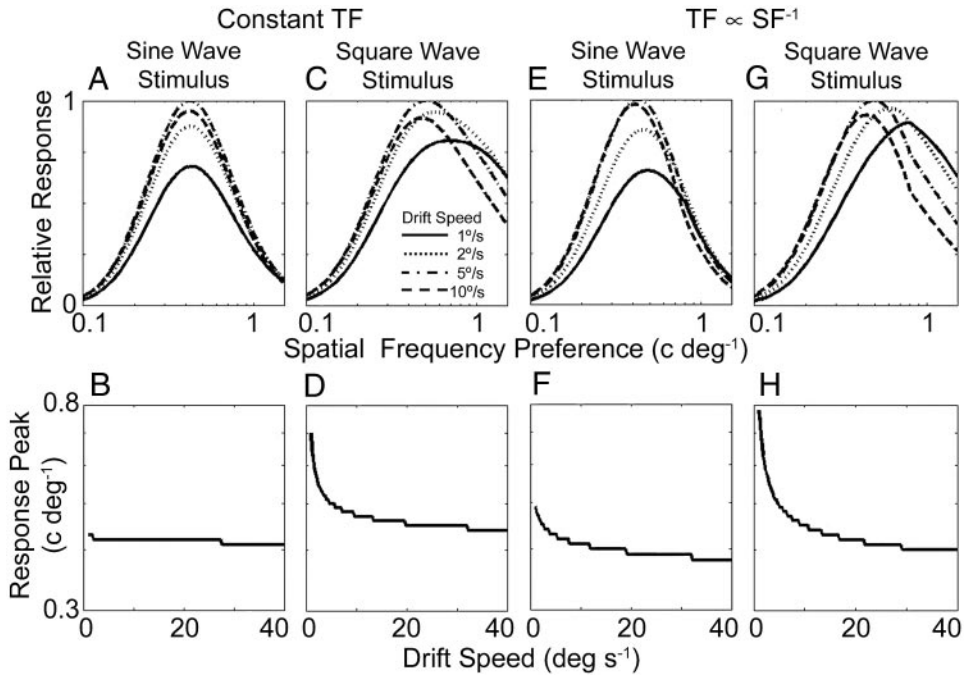

FIG. 11. Predicted effects of drift speed on responses in spatial frequency domains of cat Area 17. Plots in *A–D* assume that temporal frequency is constant across all spatial frequency domains. Plots in *E–H* assume that temporal frequency is inversely proportional to spatial frequency preference (as schematized in Fig. 13). *A*: predicted responses in different spatial frequency domains to a 0.4 c/° sine wave grating. Each trace is for a different drift speed (1°/s, solid line; 2°/s, dotted line; 5°/s, dash-dot line; 10°/s, dashed line). *B*: changing the drift speed of a sine wave grating should not substantially change which spatial frequency domains are activated. *C*: predicted responses in different spatial frequency domains to a 0.4 c/° square wave grating. *D*: high spatial frequency domains are less strongly activated when a stimulus drifts quickly than when it drifts slowly. As a result, the peak spatial frequency domain activated by a square wave shifts lower as drift speed increases. *E*: as in *A*, but assuming an inverse relationship between temporal frequency (TF) and spatial frequency (SF) preference. *F*: with an inverse relationship between temporal and spatial frequency tuning, changing drift speeds should cause a slightly different set of spatial frequency domains to be activated by the same sine wave grating. *G*: as in *C*. *H*: as in *D*. Shift in peak response to lower spatial frequencies is accentuated when temporal frequency preference is higher in low spatial frequency domains than in high spatial frequency domains.

guishable from sine wave gratings of the same frequency (Fig. 11, *A–D*).

Because of the relatively wide range of spatial frequency preferences within a cat Area 17 hypercolumn (0.2–1.5 c/°), a variety of orientations can be activated strongly by a complex stimulus such as a moving texture. More importantly, transitions among orientation domains can happen at different drift speeds for the different spatial frequency domains. As previously shown (Fig. 7), a texture drifting perpendicular to the long axis of its bars will be encoded in one orientation domain at slow speeds, and the orthogonal orientation domain at high speeds. Figure 12 shows that this transition happens at different speeds in different spatial frequency domains. The speed required for the transition increases with aspect ratio in both low and high spatial frequency domains, but the slope differs among the spatial frequency domains (Fig. 12, filled symbols). Low spatial frequency domains are more resistant to the transition than are high spatial frequency domains.

Effect of variations in temporal frequency tuning

In the previous section, we assumed that temporal frequency preference is constant across spatial frequency domains. In young cats, this seems to be the case; De Angelis et al. (1993a) found that temporal frequency preference seems to be independent of spatial frequency tuning in cats younger than 8 wk old. In adult cats, however, temporal frequency preference is inversely proportional to spatial frequency preference (Baker 1990; DeAngelis et al. 1993a). In this section, we studied how the relationship between temporal frequency and spatial frequency preferences, schematized in Fig. 13, should affect population responses.

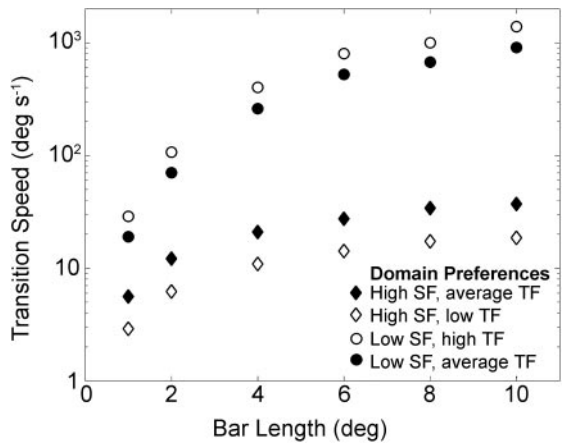

FIG. 12. Transition speed depends on spatial frequency and temporal frequency preferences. Transition speed, defined as in Fig. 7, indicates the speed of texture motion at which there is an abrupt 90° shift in the orientation domains that are activated. Transition speeds are plotted for domains with low (circles) and high (diamonds) spatial frequency preference. Stimulus textures are composed of bars 1° wide with the bar length indicated. Filled symbols represent domains in young cats, in which temporal frequency preference is constant across spatial frequency domains. Open symbols represent domains in adult cats in which temporal frequency preference is inversely proportional to spatial frequency preference.

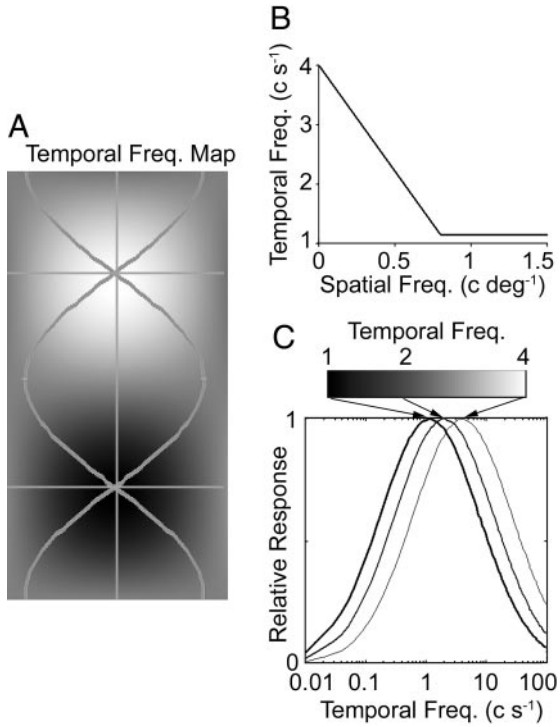

FIG. 13. Organization of filtering properties within a cat Area 17 hypercolumn, assuming that temporal frequency preference depends on spatial frequency preference. *A*: temporal frequency preference (grayscale) varies within a hypercolumn and is inversely related to the spatial frequency map (Fig. 10*A*). Superimposed on the temporal frequency map are iso-orientation lines. *B*: temporal frequency preference is inversely related to spatial frequency preference over a wide range of spatial frequencies. We assume that temporal frequency preference does not fall below 1.15 c/s, so temporal frequency preference is constant above 0.8 c/° (modeled after Fig. 14*A* of DeAngelis et al. 1993a). *C*: temporal frequency tuning curves for different locations in the temporal frequency map.

The inverse relationship between temporal and spatial frequency preferences means that speed-dependent transitions among spatial frequency domains are accentuated. For example, the peak response to a square-wave grating is in lower spatial frequency domains when temporal and spatial frequency tuning properties are inversely related (compare high drift speed points in Fig. 11, *D* and *H*). Somewhat surprisingly, there is also a shift to low spatial frequency domains when the drift speed of sine-wave gratings increases (Fig. 11, *E* and *F*). Because low spatial frequency domains respond to higher temporal frequencies, they maintain their responses to midrange spatial frequencies at speeds at which high spatial frequency domains have stopped responding. This means that quickly moving, midrange spatial frequency image components might activate low spatial frequency domains more strongly than they activate high spatial frequency domains. Therefore changing image drift speed should even change how a pure sine wave grating is encoded in different spatial frequency domains.

Orientation responses should also be affected by the relationship between temporal and spatial frequency preferences. For example, the transitions between orientation domains shown in Fig. 12 depend on temporal frequency tuning. Because low spatial frequency domains in the adult cat have a high temporal frequency cut-off, they should be more resistant to the transition than low spatial frequency domains in young cats (cf. ○ and ● in Fig. 12). Conversely, because high spatial frequency domains in the adult have a low temporal frequency cut-off, they are expected to be more sensitive to drift speed (cf. ◇ and ◆ in Fig. 12).

DISCUSSION

Previous mappings of the primary visual cortex have shown the existence of functional domains selective for features of the local spatial Fourier transform of a stimulus, namely orientation and spatial frequency. However, the experiments of Basole et al. (2003) showed that these two spatial variables are not enough to describe distributed cortical responses to moving images. We showed that the combined organization of spatial and temporal tuning properties in ferret can account for distributed population responses to both grating stimuli and more complex stimuli such as drifting bar textures. This result is consistent with the preliminary report of Mante and Carandini (2003, 2004). We also used the spatio-temporal filtering model to make predictions about activity patterns in cat Area 17, in which spatial and temporal tuning properties are distributed differently than in ferret V1.

Implications for cortical mapping

These simulations reconcile the traditional idea that stimulus parameters are represented more or less independently across the cortical surface with the findings of Basole et al. (2003) that suggest that there is a single map of spatio-temporal energy that determines cortical responses to moving images. The spatio-temporal map of the cortex can be characterized by combining the traditionally defined maps of orientation and spatial frequency preference with a map of temporal frequency preference.

Each point on the cortical surface encodes a small range of spatial frequencies and orientations in a stimulus—if this combination of spatial frequency and orientation does not exist in the stimulus, that part of cortex will not be activated, regardless of the speed or angle at which an image moves. However, even if a specific component is present in the stimulus, it may not be represented if it is moving too quickly or too slowly to fall within the temporal frequency band-pass of the visual cortex.

It is useful to consider cortical maps as maps of receptive field parameters rather than stimulus features (Issa and Stryker 2004). The average receptive field properties of a cortical domain determine the spatio-temporal tuning curves measured in response to drifting gratings. Activity in a given domain signals the presence of a specific combination of features in the stimulus that are consistent with the spatio-temporal receptive field properties of the domain.

How complex images are represented in different primary visual areas depends on the structure of the cortical maps in the different species. One surprising result from measurements in ferret primary visual cortex was that population responses to drifting textures looked like responses generated by grating stimuli (Basole et al. 2003). The model presented here suggests that this should only be the case in species in which spatial frequency preference does not vary across the cortical surface. A simple explanation for the ferret results of Basole et al. (2003) is that spatial frequency preference does not vary

significantly across the small area of cortical surface sampled. If spatial frequency preference does not vary significantly on the scale of a hypercolumn in ferret Area 17, only stimulus orientations would be encoded in spatially segregated domains.

However, in a primary visual area in which spatial frequency preference varies systematically across the cortical surface, as is the case in cat Area 17, complex stimuli should recruit different domains than do sine wave gratings. For example, square wave gratings should stimulate a wider range of spatial frequency domains than do sine wave gratings. The tangential organization of spatial frequency preference provides a second variable with which stimulus information can be encoded by position on the cortical surface.

Describing the organization of cortex in terms of maps of separable tuning properties simplifies the job of predicting responses to complex stimuli. If, for example, the tuning curves are not separable one would have to measure responses to every combination of spatial frequency, orientation, and temporal frequency to characterize the spatio-temporal responses of cortex. If we need n measurements to densely sample one dimension (for example, 8 orientations to sample all orientations), we would need n^3 measurements to specify the spatio-temporal response properties of any point. If, however, you can assume separability, only $3n$ measurements are needed: n orientations for the orientation tuning curve, n for spatial frequency, and n for temporal frequency. Because a model of separable tuning curves predicts the responses presented in Basole et al. (2003), mapping the cortical organization of tuning properties is a simple way to summarize the cortical responses to complex images.

Model assumptions and limitations

This linear model ignores several aspects of cortical organization that may contribute to the distributed responses to moving images. For example, maps of direction selectivity have been found in ferret Area 17 (Weliky et al. 1996) and cat Area 18 (Shmuel and Grinvald 1996) but are not incorporated in our model. Our simulations show that direction selectivity is not necessary to characterize the cortical responses to texture stimuli measured in ferret Area 17 (Basole et al. 2003). Ocular dominance columns are also ignored, because the structure of both the orientation and spatial frequency maps are the same whether constructed using monocular or binocular stimuli (Crair et al. 1997; Hubener et al. 1997; Issa et al. 2000).

The effects of several well-described nonlinearities in cortical responses (reviewed in Carandini et al. 1999; Dayan and Abbott 2001; De Valois and De Valois 1990) are not considered in this analysis. Some of the nonlinearities, for example, the compressive nonlinearity that describes response saturation with increasing contrast, would change response amplitudes but not the pattern of activity across functional domains. Other nonlinearities, however, will alter the pattern of activity. Specifically, suppression of cortical responses has been characterized for stimuli containing multiple orientations or multiple spatial frequencies (Bonds 1989; Ringach et al. 2002). In ongoing experiments, we are studying the effects of these nonlinearities on the distributed pattern of cortical responses.

The quantitative match between our simulations and the measurements of Basole et al. (2003) rely on the estimated spatio-temporal parameters for the ferret. One recent study that measured temporal frequency tuning in 32 neurons in ferret Area 17 (Alitto and Usrey 2004) found several neurons with a peak temporal frequency near our estimate; however, the majority of units had a lower peak temporal frequency than we estimated. Different temporal frequency tuning properties would affect the magnitude of the shifts. For example, a lower average temporal frequency preference would produce a lower crossing speed than shown in Fig. 4. However, the qualitative trends presented in Figs. 3–7 would be preserved.

Implications for psychophysics

The spatio-temporal energy model has been used to predict a variety of psychophysical phenomena. Combining the model with a description of cortical organization allows us to predict the distributed responses that correspond to such phenomena.

Psychophysical experiments show that visual acuity changes with image speed (dynamic acuity, Brown 1972; Chung and Bedell 2003; Levi 1996; Westheimer and McKee 1975). As the speed of image motion increases, less detail is perceived. The predictions shown in Fig. 11 suggest that increasing drift speed should shift cortical responses to lower spatial frequency domains. If these predictions are born out experimentally, they will confirm the hypothesis that the tuning properties of primary visual cortex limit dynamic acuity.

Motion streaks are another perceptual phenomenon associated with quickly moving images—the streaks are perceived as lines trailing a moving object. Motion streaks can be used by observers to determine motion direction (Geisler 1999), and individual neurons in V1 can respond to a quickly moving dot as though presented with a bar oriented along the axis of motion (Geisler et al. 2001). The 90° flip in peak orientation response observed by Basole et al. (2003) and simulated in Figs. 5, 7, and 12 is consistent with the perception of motion streaks. Above a certain speed, the dominant orientation encoded in the pattern of cortical activity is determined by the axis of motion, not the spatial orientation of image components.

The simulations also suggest that the speed at which these transitions occur depends on the spatial frequency and temporal frequency tuning properties of the cortical domain (as in Figs. 9 and 12). High spatial frequency channels are more susceptible to the transition than are low spatial frequency channels, even when their temporal tuning properties are identical. This suggests that motion streaks should be perceived first in high spatial frequency domains as image velocity is increased.

The effects of temporal frequency tuning on orientation domain activity should act through a similar mechanism as the spatial frequency tuning properties. That is, temporal frequency tuning restricts which spatial frequencies can contribute to cortical responses. When temporal frequency tuning is constant across spatial frequency domains, it produces a loss of high spatial frequency information at high drift speeds. With the inverse relationship between temporal frequency and spatial frequency preferences (Baker 1990; DeAngelis et al. 1993a), the loss of high spatial frequency information is accentuated. One side effect of this is that peak orientation responses in high spatial frequency domains shift at very low

speeds. The inverse relationship between spatial and temporal frequency preference has the effect of further decoupling orientation responses in different spatial frequency channels—the greater the difference in temporal frequency tuning among spatial frequency domains, the less likely it is that the same orientation domains are activated in the different spatial frequency channels.

In conclusion, a model of spatio-temporal filtering predicts that the pattern of cortical responses driven by moving images should depend on how filter parameters are mapped across the cortical surface. Six separable parameters, consisting of spatial and temporal preferences and bandwidth, specify the spatio-temporal filters. Variations in these parameters define the standard orientation and spatial frequency preference maps, along with a map of temporal frequency preference. For the simple organization of filtering parameters in which only orientation preference varies, the spatio-temporal filtering model can quantitatively account for the surprising shifts observed in orientation domains activated in response to drifting textures (Basole et al. 2003). In addition, the model predicts qualitatively different activation patterns for visual cortical areas that differ in how spatial frequency and temporal frequency tuning properties are mapped.

ACKNOWLEDGMENTS

We thank the Fitzpatrick laboratory for comments on an early draft of this paper. P. Ulinski, R. McCrea, M. Sherman, J. Cowan, and members of the Issa laboratory provided helpful comments and discussion. V. Mante and M. Carandini, working independently, have obtained results similar to ours. We thank them for coordinating with us the publication of their paper.

GRANTS

T. I. Baker is supported by the Burroughs Wellcome Fund Interfaces Fellowship 1001774. This work was supported by grants from the Brain Research Foundation and Mallinckrodt Foundation.

REFERENCES

Adelson EH and Bergen JR. Spatiotemporal energy models for the perception of motion. *J Opt Soc Am A* 2: 284–299, 1985.

Alitto HJ and Usrey WM. Influence of contrast on orientation and temporal frequency tuning in ferret primary visual cortex. *J Neurophysiol* 91: 2797–2808, 2004.

Baker CL Jr. Spatial- and temporal-frequency selectivity as a basis for velocity preference in cat striate cortex neurons. *Vis Neurosci* 4: 101–113, 1990.

Baker GE, Thompson ID, Krug K, Smyth D, and Tolhurst DJ. Spatial-frequency tuning and geniculocortical projections in the visual cortex (areas 17 and 18) of the pigmented ferret. *Eur J Neurosci* 10: 2657–2668, 1998.

Basole A, White LE, and Fitzpatrick D. Mapping multiple features in the population response of visual cortex. *Nature* 424: 986–990, 2003.

Basole A, White LE, and Fitzpatrick D. Mapping of Spatial and Temporal Frequency Preference in ferret visual cortex. *Soc Neurosci Abst* 410.415, 2004.

Bonds AB. Role of inhibition in the specification of orientation selectivity of cells in the cat striate cortex. *Vis Neurosci* 2: 41–55, 1989.

Bonhoeffer T and Grinvald A. Iso-orientation domains in cat visual cortex are arranged in pinwheel-like patterns. *Nature* 353: 429–431, 1991.

Brown B. Resolution thresholds for moving targets at the fovea and in the peripheral retina. *Vision Res* 12: 293–304, 1972.

Carandini M, Heeger DJ, and Movshon JA. Linearity and gain control in V1 simple cells. In: *Models of Cortical Circuits*, edited by Ulinski PS, Jones EG, and Peters A. New York: Kluwer Academic/Plenum Publishers, 1999, p. 401–443.

Chapman B, Stryker MP, and Bonhoeffer T. Development of orientation preference maps in ferret primary visual cortex. *J Neurosci* 16: 6443–6453, 1996.

Chung ST and Bedell HE. Velocity dependence of Vernier and letter acuity for band-pass filtered moving stimuli. *Vision Res* 43: 669–682, 2003.

Crair MC, Ruthazer ES, Gillespie DC, and Stryker MP. Ocular dominance peaks at pinwheel center singularities of the orientation map in cat visual cortex. *J Neurophysiol* 77: 3381–3385, 1997.

Dayan P and Abbott LF. *Theoretical Neuroscience: Computational and Mathematical Modeling of Neural Systems.* Cambridge, MA: MIT Press, 2001.

DeAngelis GC, Ohzawa I, and Freeman RD. Spatiotemporal organization of simple-cell receptive fields in the cat's striate cortex. I. General characteristics and postnatal development. *J Neurophysiol* 69: 1091–1117, 1993a.

DeAngelis GC, Ohzawa I, and Freeman RD. Spatiotemporal organization of simple-cell receptive fields in the cat's striate cortex. II. Linearity of temporal and spatial summation. *J Neurophysiol* 69: 1118–1135, 1993b.

De Valois KK, De Valois RL, and Yund EW. Responses of striate cortex cells to grating and checkerboard patterns. *J Physiol* 291: 483–505, 1979.

De Valois RL and De Valois KK. *Spatial Vision.* Oxford: Oxford Clarendon Press, 1990.

Everson RM, Prashanth AK, Gabbay M, Knight BW, Sirovich L, and Kaplan E. Representation of spatial frequency and orientation in the visual cortex. *Proc Natl Acad Sci USA* 95: 8334–8338, 1998.

Geisler WS. Motion streaks provide a spatial code for motion direction. *Nature* 400: 65–69, 1999.

Geisler WS, Albrecht DG, Crane AM, and Stern L. Motion direction signals in the primary visual cortex of cat and monkey. *Vis Neurosci* 18: 501–516, 2001.

Gizzi MS, Katz E, Schumer RA, and Movshon JA. Selectivity for orientation and direction of motion of single neurons in cat striate and extrastriate visual cortex. *J Neurophysiol* 63: 1529–1543, 1990.

Hubel DH and Wiesel TN. Ferrier lecture. Functional architecture of macaque monkey visual cortex. *Proc R Soc Lond B Biol Sci* 198: 1–59, 1977.

Hubener M, Shoham D, Grinvald A, and Bonhoeffer T. Spatial relationships among three columnar systems in cat area 17. *J Neurosci* 17: 9270–9284, 1997.

Issa NP and Stryker MP.Receptive field parameters estimated from intrinsic signal images of cat primary visual cortex. *Soc Neurosci Abst* 12.16, 2004.

Issa NP, Trachtenberg JT, Chapman B, Zahs KR, and Stryker MP. The critical period for ocular dominance plasticity in the Ferret's visual cortex. *J Neurosci* 19: 6965–6978, 1999.

Issa NP, Trepel C, and Stryker MP. Spatial frequency maps in cat visual cortex. *J Neurosci* 20: 8504–8514, 2000.

Levi DM. Pattern perception at high velocities. *Curr Biol* 6: 1020–1024, 1996.

Mante V and Carandini M. Visual cortex: seeing motion. *Curr Biol* 13: R906–R908, 2003.

Mante V and Carandini M. Energy models and the mapping of multiple features in visual cortex. *J Vis* 12a, 2004.

McLean J and Palmer LA. Contribution of linear spatiotemporal receptive field structure to velocity selectivity of simple cells in area 17 of cat. *Vision Res* 29: 675–679, 1989.

Movshon JA, Thompson ID, and Tolhurst DJ. Spatial and temporal contrast sensitivity of neurones in areas 17 and 18 of the cat's visual cortex. *J Physiol* 283: 101–120, 1978.

Rao SC, Toth LJ, and Sur M. Optically imaged maps of orientation preference in primary visual cortex of cats and ferrets. *J Comp Neurol* 387: 358–370, 1997.

Ringach DL, Bredfeldt CE, Shapley RM, and Hawken MJ. Suppression of neural responses to nonoptimal stimuli correlates with tuning selectivity in macaque V1. *J Neurophysiol* 87: 1018–1027, 2002.

Schwartz TH. Optical imaging of epileptiform events in visual cortex in response to patterned photic stimulation. *Cereb Cortex* 13: 1287–1298, 2003.

Shmuel A and Grinvald A. Functional organization for direction of motion and its relationship to orientation maps in cat area 18. *J Neurosci* 16: 6945–6964, 1996.

Shoham D, Hubener M, Schulze S, Grinvald A, and Bonhoeffer T. Spatio-temporal frequency domains and their relation to cytochrome oxidase staining in cat visual cortex. *Nature* 385: 529–533, 1997.

Tolhurst DJ and Thompson ID. Organization of neurones preferring similar spatial frequencies in cat striate cortex. *Exp Brain Res* 48: 217–227, 1982.

Tootell RB, Silverman MS, and De Valois RL. Spatial frequency columns in primary visual cortex. *Science* 214: 813–815, 1981.

van Santen JP and Sperling G. Elaborated Reichardt detectors. *J Opt Soc Am A* 2: 300–321, 1985.

Watson AB and Ahumada AJ Jr. Model of human visual-motion sensing. *J Opt Soc Am A* 2: 322–341, 1985.

Weliky M, Bosking WH, and Fitzpatrick D. A systematic map of direction preference in primary visual cortex. *Nature* 379: 725–728, 1996.

Weliky M, Kandler K, Fitzpatrick D, and Katz LC. Patterns of excitation and inhibition evoked by horizontal connections in visual cortex share a common relationship to orientation columns. *Neuron* 15: 541–552, 1995.

Westheimer G and McKee SP. Visual acuity in the presence of retinal-image motion. *J Opt Soc Am* 65: 847–850, 1975.

Yu H-B, Farley BJ, and Sur M. Spatial relationships between retinotopy and four other feature maps in ferret visual cortex. *Soc Neurosci Abst*, 159.13, 2002.

Zhang J and Issa NP. Dynamic visual acuity and activation patterns of spatial frequency domains of primary visual cortex. *Soc Neurosci Abst*, 648.6, 2004.